

Supporting Information

For

Carbide Complexes as π -Acceptor Ligands

Anders Reinholdt, Johan E. Vibenholt, Thorbjørn J. Morsing, Magnus Schau-Magnussen, Nini E. A. Reeler, and Jesper Bendix*

Department of Chemistry, University of Copenhagen, Universitetsparken 5, DK-2100, Denmark

Telephone: +45 35320101; Email: bendix@kiku.dk

Contents

Materials and methods

Syntheses	S3
Physical measurements	S9
Supporting figures.....	S14
Figure S 1 ^1H -NMR spectrum of 11 .	
Figure S 2 ^1H -NMR spectrum (zoom: 1.0 – 2.9 ppm) of 11 .	
Figure S 3 $^{13}\text{C}\{^1\text{H}\}$ -NMR spectrum of ^{13}C -labelled 11 .	
Figure S 4 $^{31}\text{P}\{^1\text{H}\}$ -NMR spectrum of 11 .	
Figure S 5 $^{13}\text{C}\{^1\text{H}\}$ -NMR spectrum, 348 – 353 ppm; conversion of 6 to 7 with pyridine.	
Figure S 6 $^{13}\text{C}\{^1\text{H}\}$ -NMR spectrum, 118 – 155 ppm; conversion of 6 to 7 with pyridine.	
Figure S 7 $^{13}\text{C}\{^1\text{H}\}$ -NMR spectrum; conversion of 11 to 1 with $[\text{RhCl}(\text{cod})]_2$.	
Figure S 8 $^{13}\text{C}\{^1\text{H}\}$ -NMR spectrum; conversion of 11 to 2 with $[\text{IrCl}(\text{cod})]_2$.	
Figure S 9 $^{13}\text{C}\{^1\text{H}\}$ -NMR spectrum; conversion of 11 to 3 with $[\text{RhCl}(\text{CO})_2]_2$.	
Figure S 10 $^{13}\text{C}\{^1\text{H}\}$ -NMR spectrum; conversion of 11 to 6 with $(\text{AsPh}_4)[\text{PtCl}_3(\text{C}_2\text{H}_4)]$.	
Figure S 11 Raman spectra of RuC with ^{12}C and ^{13}C as terminal carbide ligand.	
Figure S 12 Raman spectra of 11 with ^{12}C and ^{13}C as carbide bridge.	
Figure S 13 IR spectrum of 3 .	
Figure S 14 IR spectrum of 4 .	
Figure S 15 Histograms with M-C distances (M = Rh, Ir, Pd, Pt, Ag, Au).	
References.....	S23

Materials and methods

Syntheses: Unless otherwise stated, no attempts were made to exclude air in the syntheses of **1** – **12**. Acetone (technical), chloroform (Sigma-Aldrich, HPLC, $\geq 99.8\%$), chloroform-*d* (Sigma-Aldrich, 99.8% D), dichloromethane (Sigma-Aldrich, HPLC, $\geq 99.8\%$), dichloromethane-*d2* (Sigma-Aldrich, 99.9% D), diethyl ether (VWR Chemicals), hexane (Sigma-Aldrich, HPLC, $\geq 97.0\%$), pentane (Sigma-Aldrich, HPLC, $\geq 99.0\%$), toluene (technical, VWR Chemicals), and petroleum ether (VWR Chemicals, boiling point 40–65 °C) were bought from commercial suppliers and used as received. [Ru(C)Cl₂(PCy₃)₂] (**RuC**) was synthesized according to the published procedure (Johnson¹); **Ru**¹³C was obtained with ¹³CH₂¹³CHOAc (Sigma-Aldrich, 99% ¹³C). [RhCl(cod)]₂,² [IrCl(cod)]₂,³ [RhCl(CO)₂]₂,⁴ (PNP)[IrCl₂(CO)₂],⁵ (AsPh₄)[PtCl₃(C₂H₄)],⁶ *trans*-[PtCl₂(C₂H₄)(py)],⁷ *cis*-[PtCl₂(dms-*S*)₂],⁸ [Ag(4-Ph-terpy)]OTf,⁹ [AuCl(SC₄H₈)],¹⁰ and [AuCl(PPh₃)]¹¹ were prepared according to published procedures. (PNP)₂[Pd₂Cl₆]¹² (PNP⁺ replacing AsPh₄⁺), [Ag(tht)₂]OTf¹³ (OTf⁻ replacing ClO₄⁻), and [Ag(4-Ph-terpy)]OTf⁹ (terpy replacing 4'-Ph-terpy) were prepared by the obvious modifications of published procedures.

Synthesis of [(Cy₃P)₂Cl₂RuC-RhCl(cod)] (1). [RhCl(cod)]₂ (12.7 mg, 25.8 μmol) and **RuC** (38.4 mg, 51.6 μmol) were dissolved in 2 ml CH₂Cl₂ and stirred for 10 minutes. The solution was concentrated to 0.5 ml, and 3 ml pentane was added. Under a stream of N₂, the solution was evaporated to dryness and the orange residue was dried *in vacuo*. ¹H-NMR shows the product to contain dichloromethane and pentane. Yield (**1** · ¼ CH₂Cl₂ · ½ pentane): 53.6 mg, 51.1 μmol, 99.1% based on **RuC**. Crystals suitable for X-ray crystallography were grown from a CH₂Cl₂ solution layered with pentane. ¹H-NMR, 500 MHz, CDCl₃, δ: 5.44 (d, *J* = 5.9 Hz, 2H), 4.06 (d, *J* = 5.0 Hz, 2H), 2.78 – 2.64 (m, 6H), 2.52 – 2.30 (m, 4H), 2.29 – 2.19 (m, 12H), 2.15 – 2.03 (m, 4H), 1.97 – 1.82 (m, 18H), 1.82 – 1.68 (m, 12H), 1.37 – 1.23 (m, 18H). ¹³C{¹H}-NMR, 126 MHz, CDCl₃, δ: 411.71 (dt, *J* = 58.9, 5.9 Hz), 112.66, 74.64 (d, *J* = 12.6 Hz), 33.05 (t, *J* = 9.4 Hz), 32.46, 30.15 (broad s), 28.66, 28.16 (t, *J* = 4.8 Hz), 26.69. ³¹P{¹H}-NMR, 121 MHz, CDCl₃, δ: 34.63 (d, *J* = 5.4 Hz). Anal. Calc. for C₄₅H₇₈Cl₃P₂RhRu · ¼ CH₂Cl₂ · ½ CH₃(CH₂)₃CH₃: C: 54.69%, H: 8.12%. Found: C: 54.28%, H: 8.11%.

Synthesis of [(Cy₃P)₂Cl₂RuC-IrCl(cod)] (2). Under an N₂-atmosphere, [IrCl(cod)]₂ (13.1 mg, 19.5 μmol) and RuC (29.1 mg, 39.1 μmol) were dissolved in 1 ml CH₂Cl₂ resulting in a deep red solution. The solution was stirred for 10 minutes, 6 ml hexane was added, and the solution was concentrated under a slow stream of N₂ over 12 hours. Red crystals of **2** were separated from the mother liquor by decanting, washed once with hexane (3 ml), and dried *in vacuo*. Yield: 36.6 mg, 33.9 μmol, 86.7% based on RuC. Crystals suitable for X-ray crystallography were grown by slow evaporation from a 1:1 CH₂Cl₂-petroleum ether solution. ¹H-NMR, 500 MHz, CDCl₃, δ 5.43 (dt, *J* = 5.2, 2.3 Hz, 2H), 3.78 – 3.72 (m, 2H), 2.80 – 2.70 (m, 6H), 2.36 – 2.15 (2 m, 4 H + 12H), 2.04 – 1.93 (m, 4H), 1.92 – 1.83 (m, 12H), 1.83 – 1.65 (m, 18H), 1.36 – 1.24 (m, 18H). ¹³C{¹H}-NMR, 126 MHz, CDCl₃, δ: 387.66 (t, *J* = 6.0 Hz), 106.93 (d, *J* = 3.0 Hz), 57.32, 33.21, 32.98 (t, *J* = 9.4 Hz), 30.11 (broad s), 29.30, 28.14 (t, *J* = 4.8 Hz), 26.69. ³¹P{¹H}-NMR, 121 MHz, CDCl₃, δ: 34.25 (d, *J* = 5.7 Hz). Anal. Calc. for C₄₅H₇₈Cl₃IrP₂Ru: C: 50.01%, H: 7.28%. Found: C: 49.63%, H: 7.43%.

Synthesis of *trans*-[(Cy₃P)₂Cl₂RuC-RhCl(CO)]₂ (3). [RhCl(CO)₂]₂ (11.1 mg, 28.6 μmol) and RuC (42.5 mg, 57.1 μmol) were dissolved in 1.5 ml CHCl₃ with concomitant evolution of CO gas. An orange powder formed, which was dissolved as the volume was increased to 25 ml. Remaining solids, were removed by micro filtration, and diethyl ether was allowed to diffuse into the filtrate for 26 days. Orange crystals of **3** were separated by decanting, washed twice with diethyl ether (2 x 10 ml), and air dried. Yield: 34.6 mg, 19.0 μmol, 66.5% based on RuC. Crystals suitable for X-ray crystallography were grown by this procedure. ¹H-NMR, 500 MHz, CDCl₃, δ: 2.76 – 2.65 (m, 6H), 2.38 – 2.27 (m, 12H), 1.95 – 1.86 (m, 12H), 1.79 – 1.73 (m, 6H), 1.73 – 1.62 (m, 12H), 1.35 – 1.22 (m, 18H). ¹³C{¹H}-NMR, 126 MHz, CDCl₃, δ: 397.60 (dt, *J* = 60.0, 7.5 Hz), 178.88 (d, *J* = 86.1 Hz), 32.51 (t, *J* = 9.5 Hz), 30.50, 28.07 (t, *J* = 5.0 Hz), 26.78. ³¹P{¹H}-NMR, 121 MHz, CDCl₃, δ: 35.52. FAB-MS (NBA matrix): *m/z* calc. for [(Cy₃P)₂Cl₂RuC-RhCl(CO)]₂ – Cl + H⁺: 1787.4; found: 1787.3. Anal. Calc. for C₇₆H₁₃₂Cl₆O₂P₄Rh₂Ru₂: C: 50.09%, H: 7.30%. Found: C: 50.08%, H: 7.35%. IR (solid **3**; ν/cm⁻¹): 2022 (CO).

Synthesis of *trans*-{[(Cy₃P)₂Cl₂RuC]₂IrCl(CO)} (4). Note: (PNP)Cl is soluble in acetone. *cis*-(PNP)[IrCl₂(CO)₂] (11.3 mg, 13.2 μmol) and RuC (19.6 mg, 26.3 μmol) were dissolved in 5 ml chloroform resulting in a clear yellow solution in which a yellow precipitate formed over the next two hours. The solvent was removed under a stream of N₂, and the residue was washed with acetone (2 x 10 ml). The resulting yellow powder of **4** was dried *in vacuo*. Yield: 21.5 mg, 12.3 μmol, 93.6% based on

RuC. Crystals suitable for X-ray crystallography were grown by diffusion of diethyl ether into a chloroform solution of **4**. $^1\text{H-NMR}$, 300 MHz, CDCl_3 , δ : 2.77 – 2.60 (m, 6H), 2.32 – 2.16 (m, 12H), 1.93 – 1.80 (m, 12H), 1.77 – 1.55 (m, 18H), 1.37 – 1.12 (m, 18H). $^{13}\text{C}\{^1\text{H}\}$ -NMR, 126 MHz, CDCl_3 , δ : 397.42, 167.23, 32.71 (t, $J = 9.5$ Hz), 30.29, 28.04 (t, $J = 5.1$ Hz), 26.71. $^{31}\text{P}\{^1\text{H}\}$ -NMR, 121 MHz, CDCl_3 : δ 36.21. ESI+ MS (CH_3CN , HCO_2H), m/z , calc. for $[(\text{Cy}_3\text{P})_2\text{Cl}_2\text{RuC}]_2\text{IrCl}(\text{CO}) - \text{Cl} + \text{CH}_3\text{CN}]^+$ 1750.60; found 1750.60. Anal. Calc. for $\text{C}_{75}\text{H}_{132}\text{Cl}_5\text{IrOP}_4\text{Ru}_2$: C: 51.61%, H: 7.62%; found: 51.60%, H: 7.83%. IR (solid **4**; ν/cm^{-1}): 1990 (CO).

Synthesis of (PNP)[(Cy₃P)₂Cl₂RuC-PdCl₃] (5). Formation of **5** should be carried out in CH_2Cl_2 as $(\text{PNP})_2[\text{Pd}_2\text{Cl}_6]$ is sparingly soluble in CHCl_3 . $(\text{PNP})_2[\text{Pd}_2\text{Cl}_6]$ (10.4 mg, 6.92 μmol) and **RuC** (10.3 mg, 13.8 μmol) were stirred in 0.8 ml boiling CH_2Cl_2 until the solids dissolved (20 minutes). The solution was layered with diethyl ether, and after a week, orange crystals of **5** were collected, washed with diethyl ether (2 x 5 ml), and dried *in vacuo*. Yield: 13.8 mg, 9.22 μmol , 66.7% based on **RuC**. Crystals suitable for X-ray crystallography were grown from a CHCl_3 solution by diffusion of diethyl ether vapor. $^1\text{H-NMR}$, 300 MHz, CD_2Cl_2 , δ : 7.72 – 7.63 (m, 6H), 7.55 – 7.40 (m, 24H), 2.77 – 2.61 (m, 6H), 2.42 – 2.29 (m, 12H), 1.92 – 1.79 (m, 12H), 1.78 – 1.56 (m, 18H), 1.36 – 1.17 (m, 18H). $^{13}\text{C}\{^1\text{H}\}$ -NMR, 126 MHz, CD_2Cl_2 , δ : 381.07 (t, $J = 5.6$ Hz), 134.32, 132.84 – 132.56 (m), 130.23 – 129.89 (m), 127.59 (d, $J = 107.5$ Hz), 33.04 (t, $J = 9.7$ Hz), 30.68, 28.59 (t, $J = 5.3$ Hz), 27.21. $^{31}\text{P}\{^1\text{H}\}$ -NMR, 121 MHz, CD_2Cl_2 , δ : 39.58, 22.15. ESI- MS (CH_3CN , HCO_2H), m/z , calc. for $[(\text{Cy}_3\text{P})_2\text{Cl}_2\text{RuCPdCl}_3 - \text{Cl} + \text{HCO}_2]^-$, $[(\text{Cy}_3\text{P})_2\text{Cl}_2\text{RuCPdCl}_3]^-$: 967.14, 957.12; found: 967.16, 957.13. Anal. Calc. for $\text{C}_{73}\text{H}_{96}\text{Cl}_5\text{NP}_4\text{PdRu}$: 58.60%, H: 6.47%, N: 0.94%; found C: 58.62%, H: 6.54%, N: 0.93%.

Synthesis of (AsPh₄)[(Cy₃P)₂Cl₂RuC-PtCl₃] (6). $(\text{AsPh}_4)[\text{PtCl}_3(\text{C}_2\text{H}_4)]$ (7.6 mg, 11 μmol) and **RuC** (8.0 mg, 11 μmol) were stirred in 0.5 ml CH_2Cl_2 for 30 minutes. The solution was layered with 2 ml pentane. After 2 days, orange crystals of **6** were separated from the mother liquor and washed with pentane (1 x 2 ml). Yield: 9.1 mg, 6.4 μmol , 59% based on **RuC**. Crystals suitable for X-ray crystallography may be grown by this method or with toluene in place of pentane. $^1\text{H-NMR}$, 500 MHz, CDCl_3 , δ : 7.85 – 7.78 (m, 12H), 7.69 – 7.63 (m, 8H), 2.78 – 2.67 (m, 6H), 2.44 – 2.34 (m, 12H), 1.85 – 1.77 (m, 12H), 1.74 – 1.60 (m, 18H), 1.33 – 1.16 (m, 18H). $^{13}\text{C}\{^1\text{H}\}$ -NMR, 126 MHz, CDCl_3 , δ : 350.95 (t, $J = 7.5$ Hz and d, $J = 1395.5$ Hz), 134.83, 133.27, 131.66, 120.57, 32.89 (t, $J = 9.6$ Hz), 30.31, 28.18 (t, $J = 5.5$ Hz), 26.85. $^{31}\text{P}\{^1\text{H}\}$ -NMR, 121 MHz, CDCl_3 , δ : 33.54. ESI-MS (CH_3CN , HCO_2H) m/z : calc.

for [AsPh₄]⁺: 383.08; found.: 383.08; calc. for [(Cy₃P)₂Cl₂RuCPtCl₃]⁻: 1046.17; found: 1046.22. Anal. Calc. for C₆₁H₈₆AsCl₅P₂PtRu: C: 51.25%, H: 6.06%. Found: C: 50.76%, H: 5.91%.

Synthesis of *trans*-[(Cy₃P)₂Cl₂RuC-PtCl₂(py)] (7). *Method A:* *trans*-[PtCl₂(C₂H₄)(py)] (11.4 mg, 30.6 μmol) and **RuC** (22.8 mg, 30.6 μmol) were placed in 1 ml chloroform. After the solids dissolved, pentane was allowed to diffuse into the solution over 3 days. Orange prismatic crystals of **7** were separated by decanting, washed with pentane (3 x 3 ml) and dried *in vacuo*. Yield (**7** · CHCl₃): 32.5 mg, 26.9 μmol, 87.8% based on **RuC**. Crystals suitable for X-ray crystallography were grown by this procedure. ¹H-NMR, 500 MHz, CD₂Cl₂, δ: 8.70 – 8.57 (m, 2H), 7.81 (t, *J* = 7.7 Hz, 1H), 7.42 – 7.34 (m, 2H), 2.80 – 2.67 (m, 6H), 2.45 – 2.32 (m, 12H), 1.91 – 1.81 (m, 12H), 1.77 – 1.65 (m, 18H), 1.37 – 1.22 (m, 18H). ¹³C{¹H}-NMR, 126 MHz, CDCl₃, δ: 350.34 (t, *J* = 6.7 Hz and d, *J* = 1283.4 Hz), 152.39, 139.01, 124.98, 33.02 (t, *J* = 9.7 Hz), 30.45, 28.13 (t, *J* = 5.3 Hz), 26.72. ³¹P{¹H}-NMR, 121 MHz, CDCl₃, δ: 37.38 (d, *J* = 6.6 Hz). ESI-MS (CH₃CN, HCO₂H), *m/z*, calc. for [(Cy₃P)₂Cl₂RuCPtCl₂(py) + Hpy]⁺, [(Cy₃P)₂Cl₂RuCPtCl₂(py) – Cl + CH₃CN]⁺: 1170.30, 1094.31; found: 1170.30, 1094.31. Anal. Calc. for C₄₂H₇₁Cl₄NP₂PtRu · CHCl₃: C: 42.71%, H: 6.00%, N: 1.16%. Found: C: 42.40%, H: 5.97%, N: 1.09%.

Method B: (AsPh₄)[PtCl₃(C₂H₄)] (1.4 mg, 2.0 μmol) and **Ru**¹³C (1.5 mg, 2.0 μmol) were dissolved in 0.5 ml CDCl₃. After 5 minutes, the carbide region of the ¹³C{¹H}-NMR spectrum showed only the presence of **6**. The solution was transferred to an NMR tube containing pyridine (0.3 mg, 4 μmol). After 5 minutes, another ¹³C{¹H}-NMR spectrum showed complete conversion of **6** into **7** (corroborated by the carbide bridge signal (Figure S 5) and the signals from coordinated pyridine (Figure S 6)).

Synthesis of *cis*-[(Cy₃P)₂Cl₂RuC-PtCl₂(dmsO-S)] (8). *cis*-[PtCl₂(dmsO-S)₂] (19.9 mg, 47.1 μmol) and **RuC** (35.1 mg, 47.1 μmol) were heated in 2 ml CH₂Cl₂ until the *cis*-[PtCl₂(dmsO-S)₂] dissolved (10 minutes). The solution was filtered and layered with 10 ml pentane. After two days, orange block shaped crystals of **8** were separated by decanting, washed with pentane (4 x 3 ml) and air dried. Yield (**8** · CH₂Cl₂): 44.8 mg, 38.2 μmol, 81.0% based on **RuC**. Crystals suitable for X-ray crystallography were grown by this procedure. ¹H-NMR, 500 MHz, CDCl₃, δ: 3.45 (s, 6H), 2.80 – 2.70 (m, 6H), 2.38 – 2.30 (m, 6H), 2.18 – 2.11 (m, 6H), 1.92 – 1.80 (m, 12H), 1.77 – 1.72 (m, 6H), 1.72 – 1.57 (m, 12H), 1.37 – 1.21 (m, 18H). ¹³C{¹H}-NMR, 126 MHz, CDCl₃, δ: 344.84 (t, *J* = 6.2 Hz, and d, *J* = 1333.8 Hz), 46.10, 32.84 (t, *J* = 9.6 Hz), 30.24, 28.03 (dt, *J* = 18.2, 5.1 Hz), 26.57. ³¹P{¹H}-NMR, 121 MHz, CDCl₃, δ: 39.71 (d, *J* = 5.8 Hz). MALDI-MS: *m/z* calc. for [(Cy₃P)₂Cl₂RuC-PtCl₂(dmsO-S) – Cl – dmsO], 974.2;

found, 974.2. Anal. Calc. for $C_{39}H_{72}Cl_4OP_2PtRuS \cdot CH_2Cl_2$: C: 40.93%, H: 6.35%. Found: C: 40.83%, H: 6.35%.

Synthesis of [(Cy₃P)₂Cl₂RuC-Ag(terpy)]OTf (9). [Ag(terpy)]OTf (7.1 mg, 14 μmol) and **RuC** (10.8 mg, 14.5 μmol) were stirred in 2 ml CHCl₃ for 15 hours. The solution was centrifuged to remove excess insoluble [Ag(terpy)]OTf. Pentane was allowed to diffuse into the centrifugate for three days. Yellow crystals of **9** were separated by decanting, washed two times with pentane (2 x 10 ml), and dried *in vacuo*. Yield: 14.8 mg, 12.0 μmol, 82.6% based on **RuC**. Crystals suitable for X-ray crystallography were grown by this procedure. ¹H-NMR, 500 MHz, CDCl₃, δ: 8.52 – 8.48 (m, 2H), 8.47 – 8.41 (m, 2H), 8.40 – 8.34 (m, 3H), 8.05 (t, *J* = 7.8 Hz, 2H), 7.50 (dd, *J* = 7.6, 4.8 Hz, 2H), 2.80 – 2.69 (m, 6H), 2.26 – 2.18 (m, 12H), 1.72 – 1.62 (m, 18H), 1.62 – 1.52 (m, 12H), 1.28 – 1.17 (m, 12H), 1.17 – 1.08 (m, 6H). ¹³C{¹H}-NMR, 126 MHz, CDCl₃, δ: 433.49 (d, *J* = 187.0 Hz), 151.26, 151.15 – 150.65 (broad s, 2 similar terpy C's), 141.72, 139.64, 125.77, 123.68, 123.23, 121.09 (q, *J* = 320.5 Hz), 31.76 (t, *J* = 10.0 Hz), 30.16, 27.88 (d, *J* = 6.1 Hz), 26.50. ³¹P{¹H}-NMR, 121 MHz, CDCl₃, δ: 44.20. ¹⁹F-NMR, 282 MHz, CDCl₃, δ: –78.44. FAB-MS (NBA matrix): *m/z* calc. for [(Cy₃P)₂Cl₂RuC-Ag(terpy) + H]⁺: 1087.3; found: 1087.41. Anal. Calc. for C₅₃H₇₇AgCl₂F₃N₃O₃P₂RuS: C: 51.54%, H: 6.28%, N: 3.40%. Found: C: 51.15%, H: 6.26%, N: 3.38%.

Synthesis of [(Cy₃P)₂Cl₂RuC-Ag(4'-Ph-terpy)]OTf (10). [Ag(4'-Ph-terpy)]OTf (25.5 mg, 45.0 μmol) and **RuC** (33.5 mg, 45.0 μmol) were stirred in 5 ml CHCl₃ for 1.5 hours. The solution was centrifuged to remove excess insoluble [Ag(4'-Ph-terpy)]OTf. Pentane was allowed to diffuse into the centrifugate for three days. Yellow crystals of **10** were separated by decanting, washed once with pentane (10 ml), and air dried. Yield: 54.2 mg, 41.3 μmol, 91.9% based on **RuC**. Crystals suitable for X-ray crystallography were grown by this procedure. ¹H-NMR, 500 MHz, CDCl₃, δ: 8.53 (s, 1H), 8.52 (s, 5H), 8.13 (t, *J* = 7.8 Hz, 2H), 7.94 (d, *J* = 7.5 Hz, 2H), 7.54 (q, *J* = 7.8 Hz, 4H), 7.48 (t, *J* = 7.3 Hz, 1H), 2.81 – 2.69 (m, 6H), 2.30 – 2.16 (m, 12H), 1.76 – 1.63 (m, 18H), 1.63 – 1.52 (m, 12H), 1.31 – 1.18 (m, 12H), 1.17 – 1.06 (m, 6H). ¹³C{¹H}-NMR, 126 MHz, CDCl₃, δ: 433.36 (d, *J* = 187.8 Hz), 153.66, 152.04, 151.07, 150.86, 139.80, 136.45, 130.50, 129.69, 127.72, 125.90, 123.38, 121.18, 121.16 (q, *J* = 320.7 Hz), 31.76 (t, *J* = 10.0 Hz), 30.21, 27.89 (t, *J* = 5.7 Hz), 26.48. ³¹P{¹H}-NMR, 121 MHz, CDCl₃, δ: 44.21. ¹⁹F-NMR, 282 MHz, CDCl₃, δ: –78.46. FAB-MS (NBA matrix): *m/z* calc. for [(Cy₃P)₂Cl₂RuC-

$\text{Ag}(4^{\text{t}}\text{-Ph-terpy}) + \text{H}]^+$: 1163.4; found: 1163.8. Anal. Calc. for $\text{C}_{59}\text{H}_{81}\text{AgCl}_2\text{F}_3\text{N}_3\text{O}_3\text{P}_2\text{RuS}$: C: 54.05%, H: 6.23%, N: 3.20%. Found: C: 53.58%, H: 6.02%, N: 3.21%.

Synthesis of $[(\text{Cy}_3\text{P})_2\text{Cl}_2\text{RuC-AuCl}]$ (11**).** $[\text{AuCl}(\text{SC}_4\text{H}_8)]$ (50.3 mg, 157 μmol) and **RuC** (116.9 mg, 156.9 μmol) were stirred in 3 ml CHCl_3 for 30 minutes. The solution was centrifuged to remove remaining insoluble substances. Diethyl ether was allowed to diffuse into the centrifugate for three days. Bright yellow crystals of **11** were separated by decanting, washed twice with diethyl ether (2 x 10 ml), and air dried. Yield: 135.6 mg, 138.8 μmol , 88.4 % based on **RuC**. Crystals suitable for X-ray crystallography were grown by this procedure. $^1\text{H-NMR}$, 500 MHz, CDCl_3 , δ : 2.74 – 2.62 (m, 6H), 2.23 – 2.11 (m, 12H), 1.94 – 1.84 (m, 12H), 1.79 – 1.72 (m, 6H), 1.66 – 1.55 (m, 12H), 1.34 – 1.19 (m, 18H). $^{13}\text{C}\{^1\text{H}\}$ -NMR, 126 MHz, CDCl_3 , δ : 395.40 (t, $J = 6.1$ Hz), 32.28 (t, $J = 9.8$ Hz), 30.29, 28.05 (t, $J = 5.4$ Hz), 26.51. $^{31}\text{P}\{^1\text{H}\}$ -NMR, 121 MHz, CDCl_3 , δ : 43.86. Anal. Calc. for $\text{C}_{37}\text{H}_{66}\text{AuCl}_3\text{P}_2\text{Ru}$: C: 45.47%, H: 6.81%. Found: C: 45.14%, H: 6.92%. Raman (solid **11**; ν/cm^{-1}): 1145/1103 ($\text{Ru}\equiv^{12}\text{C-Au}/\text{Ru}\equiv^{13}\text{C-Au}$).

Synthesis of $\{[(\text{Cy}_3\text{P})_2\text{Cl}_2\text{RuC}]_2\text{Au}\}\text{OTf}$ (12**).** *Method A:* AgOTf (4.5 mg, 18 μmol) and $[\text{AuCl}(\text{PPh}_3)]$ (8.7 mg, 18 μmol) were stirred in 1 ml CHCl_3 for ten minutes with concomitant precipitation of AgCl . **RuC** (26.1 mg, 35.0 μmol) was added along with 1 ml CHCl_3 , and the mixture was heated to 40 $^\circ\text{C}$ and stirred for 30 minutes. The solution was centrifuged to remove AgCl , and the volume was increased to 5 ml. Pentane was allowed to diffuse into the centrifugate over three days. Orange prismatic crystals of **12** were separated by decanting, washed three times with pentane (3 x 5 ml), and air dried. Yield: 11.0 mg, 5.99 μmol , 34.2% based on **RuC**. Crystals suitable for X-ray crystallography were grown with AgBF_4 replacing AgOTf to obtain an anion amenable to the structural refinement. $^1\text{H-NMR}$, 500 MHz, CDCl_3 , δ : 2.74 – 2.64 (m, 12H), 2.12 – 2.01 (m, 24H), 1.92 – 1.85 (m, 24H), 1.85 – 1.78 (m, 12H), 1.62 – 1.48 (m, 24H), 1.37 – 1.26 (m, 24H), 1.24 – 1.14 (m, 12H). $^{13}\text{C}\{^1\text{H}\}$ -NMR, 126 MHz, CDCl_3 , δ : 395.32, 121.18 (q, $J = 321.0$ Hz), 32.20 (t, $J = 9.9$ Hz), 30.62, 27.92 (t, $J = 5.2$ Hz), 26.40. $^{31}\text{P}\{^1\text{H}\}$ -NMR, 121 MHz, CDCl_3 , δ : 51.11. $^{19}\text{F-NMR}$, 282 MHz, CDCl_3 , δ : -78.42. FAB-MS (NBA matrix): m/z calc. for $\{[(\text{Cy}_3\text{P})_2\text{Cl}_2\text{RuC}]_2\text{Au} + \text{H}\}^+$: 1688.6; found: 1688.4. Anal. Calc. for $\text{C}_{75}\text{H}_{132}\text{Au}_2\text{Cl}_4\text{F}_3\text{O}_3\text{P}_4\text{Ru}_2\text{S}$: C: 49.07%, H: 7.25%. Found: C: 49.08%, H: 7.39%.

Method B: $[\text{AuCl}(\text{SC}_4\text{H}_8)]$ (10.1 mg, 31.5 μmol) and $[\text{Ag}(\text{SC}_4\text{H}_8)_2]\text{OTf}$ (13.6 mg, 31.4 μmol) were dissolved in 2 ml CHCl_3 and stirred for 15 minutes, resulting in the precipitation of AgCl . **RuC** (46.9

mg, 63.0 μmol) was added, and after 15 minutes, the solution was filtered, and the volume was reduced to 1 ml. Pentane was allowed to diffuse into the filtrate over three days. Orange prismatic crystals of **12** were separated by decanting, washed with pentane (3 x 3 ml), and dried *in vacuo*. Yield: 29.3 mg, 16.0 μmol , 50.7% based on **RuC**. Anal. Calc. for $\text{C}_{75}\text{H}_{132}\text{Au}_2\text{Cl}_4\text{F}_3\text{O}_3\text{P}_4\text{Ru}_2\text{S}$: C: 49.07%, H: 7.25%. Found: C: 48.71%, H: 7.44%.

Transmetallation reactions. $[\text{AuCl}(\text{SC}_4\text{H}_8)]$ (5.4 mg, 17 μmol) and **Ru**¹³**C** were dissolved in 0.5 ml CDCl_3 , and after 15 minutes, the carbide region of the $^{13}\text{C}\{^1\text{H}\}$ -NMR spectrum showed only the resonance from ^{13}C -labelled **11**. The solution was divided in 9 aliquots and diluted to 0.5 ml with CDCl_3 (each aliquot containing 1.9 μmol **11**). Afterwards, metal complexes that afford carbide-bridged complexes were added: $[\text{RhCl}(\text{cod})]_2$ (0.5 mg, 1 μmol), $[\text{IrCl}(\text{cod})]_2$ (0.6 mg, 1 μmol), $[\text{RhCl}(\text{CO})_2]_2$ (0.4 mg, 1 μmol), $(\text{AsPh}_4)[\text{PtCl}_3(\text{C}_2\text{H}_4)]$ (1.3 mg, 1.8 μmol), $[\text{Ag}(\text{terpy})]\text{OTf}$ (0.9 mg, 2 μmol), $[\text{Ag}(4'\text{-Ph-terpy})]\text{OTf}$ (1.1 mg, 1.9 μmol), *cis*- $[\text{PtCl}_2(\text{dmsO-S})_2]$ (0.8 mg, 2 μmol), and $(\text{PNP})_2[\text{Pd}_2\text{Cl}_6]$ (1.4 mg, 0.93 μmol). The reactions involving $[\text{RhCl}(\text{cod})]_2$, $[\text{IrCl}(\text{cod})]_2$, $[\text{RhCl}(\text{CO})_2]_2$, and $(\text{AsPh}_4)[\text{PtCl}_3(\text{C}_2\text{H}_4)]$ afforded **1** (Figure S 7), **2** (Figure S 8), **3** (Figure S 9), and **6** (Figure S 10) in low spectroscopic yields. The reactions with the remaining metal complexes failed to afford other known carbide-bridged complexes than **RuC**.

Physical measurements

NMR-spectroscopy: $^{31}\text{P}\{^1\text{H}\}$ -NMR and ^{19}F -NMR spectra were recorded on a 300 MHz Varian instrument. $^{13}\text{C}\{^1\text{H}\}$ -NMR spectra were recorded on a 500MHz Bruker instrument with a cryoprobe, and ^1H -NMR spectra were recorded on a 300 MHz Varian instrument or a 500MHz Bruker instrument with a cryoprobe. For ^1H and ^{13}C , residual solvent signals were used for calibration (CDCl_3 : $\delta = 7.26$ and 77.16 ppm, CD_2Cl_2 : $\delta = 5.33$ and 54.24 ppm, for ^1H and ^{13}C , respectively). For ^{31}P and ^{19}F , the signals were referenced to the deuterium resonances arising from the solvents.

Mass spectrometric measurements were carried out on a Jeol four sector instrument (FAB, *m*-nitrobenzylalcohol as matrix) or on a Bruker Solarix XR ESI/MALDI FT-ICR MS instrument (ESI, acetonitrile added formic acid as solvent).

Elemental analyses were performed by the microanalytical services of the Department of Chemistry, University of Copenhagen.

IR spectra of solid samples of **3** and **4** were recorded with an Agilent Technologies Cary 630 FTIR instrument.

Raman experiments were performed by placing some powder on a clean cover slip on top of an Olympus IX71 microscope aligned with a 632.8 nm HeNe CW laser (Thorlabs HRR170-1). The laser source was spectrally cleaned by a narrow bandpass filter centered at 633 nm (Semrock LL01-633-25). In the microscope the laser light was reflected on a dichroic mirror (Semrock LP02-633RU-25) towards a 100X 1.3 NA immersion oil objective (Olympus UplanFL N) that focused the laser from below on the sample. The power of the laser focused at the sample was 635 μ W (approximately 230 kW/cm²). The Raman signal was collected back through the objective. A 633 nm longpass filter (Semrock LP02-633RU-25) was used to block the 632.8 nm laser light in the detection path. The Raman spectrum was recorded using a PI Acton SpectraPro SP-2356 polychromator (1200 g mm⁻¹ blazed at 500 nm) and a PI Acton SPEC-10:100B/LN_eXcelon Spectroscopy System with a back-illuminated CCD chip (1340 x 100 pixels).

X-ray crystallographic studies: single crystals of all complexes were coated with mineral oil, picked up with nylon loops, and mounted immediately in the nitrogen cold stream of the diffractometer to prevent solvent loss.

Single-crystal X-ray diffraction studies of (**1**, **3**, **6**, **8**, **9**, **10**, **11**, and **12**) were performed at 122(2) K on a Nonius KappaCCD area-detector diffractometer, equipped with an Oxford Cryostreams low-temperature device, using graphite-monochromated Mo K_{α} radiation ($\lambda = 0.71073 \text{ \AA}$), using ω and φ scans with a scan width of 1.0° and exposure times of 60 s, using the program COLLECT.¹⁴ The crystal-to-detector distance was 35.0 mm. The program EVALCCD¹⁵ was used for data reduction, and the data were corrected for absorption by integration. The structures were solved with direct methods using SHELXS¹⁶ and refined by least-squares methods using SHELXL97.¹⁷ All non-hydrogen atoms were refined anisotropically. Hydrogen atoms were located in the difference Fourier map and refined isotropically ($U_{\text{iso}} = 1.2 U_{\text{eq}}$ of the parent atom, except for methyl hydrogens which were constrained to 1.5 U_{eq} of the parent atom) and constrained riding their parent atom in a fixed geometry.

Single-crystal X-ray diffraction studies of (**2**, **4**, **5**, and **7**) were performed at 122(2) K on a Bruker D8 VENTURE diffractometer equipped with a Mo K_α high-brilliance $I\mu S$ radiation source ($\lambda = 0.71073 \text{ \AA}$), a multilayer X-ray mirror and a PHOTON 100 CMOS detector, and an Oxford Cryosystems low temperature device. The instrument was controlled with the APEX2 software package using SAINT.¹⁸ Final cell constants were obtained from least squares fits of several thousand strong reflections. Intensity data were corrected for absorption using intensities of redundant reflections with the program SADABS.¹⁹ The structures were readily solved in Olex2 using the olex2.solve²⁰ structure solution program (Charge Flipping) and refined using the olex2.refine program²¹ or SHELXL.¹⁷ All non-hydrogen atoms were refined anisotropically and hydrogen atoms were placed at calculated positions and refined as riding atoms with isotropic displacement parameters ($U_{\text{iso}} = 1.2 U_{\text{eq}}$ of the parent atom, except for methyl hydrogens which were constrained to $1.5 U_{\text{eq}}$ of the parent atom).

Disorder in solvent molecules and cyclohexyl groups was treated with appropriate choices of the EADP, ISOR, and SADI commands. CCDC numbers 1403006 – 1403017 contain the crystallographic data reported herein. These data can be obtained free of charge from The Cambridge Crystallographic Data Centre via www.ccdc.cam.ac.uk/data_request/cif. Selected crystallographic details are listed in Table S1 below.

Table S1. Crystallographic data for **1-12**

Compound	1 (CCDC 1403011)	2 (CCDC 1403009)	3 (CCDC 1403014)	4 (CCDC 1403008)
Empirical formula	$\text{C}_{46}\text{H}_{80}\text{Cl}_3\text{P}_2\text{RhRu}$	$\text{C}_{51}\text{H}_{92}\text{Cl}_3\text{IrP}_2\text{Ru}$	$\text{C}_{81.47}\text{H}_{144.4}\text{Cl}_{8.53}\text{O}_{3.16}\text{P}_4\text{Rh}_2\text{Ru}_2$	$\text{C}_{81}\text{H}_{144}\text{Cl}_{11}\text{IrO}_2\text{P}_4\text{Ru}_2$
Formula weight	1076.27	1166.80	2009.07	2058.12

Temperature / K	122(2)	122(2)	122(2)	122(2)
Crystal system	triclinic	triclinic	monoclinic	monoclinic
Space group	<i>P</i> -1	<i>P</i> -1	<i>C</i> 2/ <i>c</i>	<i>C</i> 2/ <i>c</i>
<i>a</i> / Å	10.9350(12)	10.9458(6)	32.65(2)	13.8110(18)
<i>b</i> / Å	12.9950(5)	15.8362(9)	13.40(2)	40.893(6)
<i>c</i> / Å	18.693(3)	16.7533(10)	23.89(2)	16.343(2)
α / °	78.174(4)	111.788(2)	90.00	90
β / °	75.183(12)	96.293(2)	109.79(2)	97.877(5)
γ / °	75.241(8)	99.958(2)	90.00	90
<i>V</i> / Å ³	2455.3(5)	2607.5(3)	9832(18)	9143(2)
<i>Z</i>	2	2	4	4
ρ_{calc} / g cm ⁻³	1.456	1.486	1.357	1.495
μ / mm ⁻¹	1.012	3.086	0.969	2.212
2θ range for data collection / °	3.702 to 52.744	4.224 to 50.054	2.66 to 75.98	4.27 to 52.742
Reflections collected	54616	123709	194564	71347
Independent reflections	10014 [<i>R</i> _{int} = 0.0276]	9185 [<i>R</i> _{int} = 0.0585]	26709 [<i>R</i> _{int} = 0.0503]	9355 [<i>R</i> _{int} = 0.1059]
Restraints / parameters	6 / 566	28 / 552	0 / 497	18 / 492
Goodness-of-fit on <i>F</i> ²	1.082	1.048	1.193	1.022
Final <i>R</i> indexes [<i>I</i> >= 2σ(<i>I</i>)]	<i>R</i> ₁ = 0.0194, <i>wR</i> ₂ = 0.0472	<i>R</i> ₁ = 0.0195, <i>wR</i> ₂ = 0.0409	<i>R</i> ₁ = 0.0471, <i>wR</i> ₂ = 0.1313	<i>R</i> ₁ = 0.0346, <i>wR</i> ₂ = 0.0671
Final <i>R</i> indexes [all data]	<i>R</i> ₁ = 0.0232, <i>wR</i> ₂ = 0.0504	<i>R</i> ₁ = 0.0257, <i>wR</i> ₂ = 0.0426	<i>R</i> ₁ = 0.0668, <i>wR</i> ₂ = 0.1474	<i>R</i> ₁ = 0.0605, <i>wR</i> ₂ = 0.0752
Largest diff. peak / hole / e Å ⁻³	0.73 / -0.56	0.63 / -0.52	3.07 / -0.92	0.86 / -0.66

Compound	5 (CCDC 1403007)	6 (CCDC 1403010)	7 (CCDC 1403006)	8 (CCDC 1403012)
Empirical formula	C ₇₃ H ₉₆ Cl ₃ NP ₄ PdRu	C ₆₃ H ₈₈ AsCl ₇ O ₂ P ₂ PtRu	C ₄₃ H ₇₂ Cl ₇ NP ₂ PtRu	C ₄₀ H ₇₄ Cl ₆ OP ₂ PtRuS
Formula weight	1496.10	1558.50	1209.26	1173.85
Temperature / K	122(2)	122(2)	122(2)	122(2)
Crystal system	triclinic	triclinic	triclinic	triclinic
Space group	<i>P</i> -1	<i>P</i> -1	<i>P</i> -1	<i>P</i> -1
<i>a</i> / Å	11.5671(14)	11.3070(19)	9.6223(3)	10.4320(7)
<i>B</i> / Å	13.5147(13)	13.3050(9)	14.2389(5)	12.7130(12)
<i>c</i> / Å	24.091(3)	24.398(5)	18.6464(7)	19.025(3)
α / °	76.202(4)	75.582(9)	85.8029(11)	77.214(9)
β / °	88.744(4)	88.059(13)	78.4958(10)	80.085(5)
γ / °	72.724(4)	71.085(6)	76.9593(10)	82.926(6)
<i>V</i> / Å ³	3487.6(7)	3358.5(10)	2437.81(15)	2414.3(4)
<i>Z</i>	2	2	2	2
ρ_{calc} / g cm ⁻³	1.425	1.541	1.647	1.615
μ / mm ⁻¹	0.800	3.160	3.656	3.678
2θ range for data collection / °	4.704 to 61.998	3.344 to 52.744	4.424 to 55.754	2.22 to 52.744
Reflections collected	110647	48384	30567	66702
Independent reflections	22216 [<i>R</i> _{int} = 0.0990]	13687 [<i>R</i> _{int} = 0.0628]	11589 [<i>R</i> _{int} = 0.0455]	9858 [<i>R</i> _{int} = 0.0279]
Restraints / parameters	0 / 766	12 / 753	0 / 503	0 / 471
Goodness-of-fit on <i>F</i> ²	1.025	1.044	1.037	1.171
Final <i>R</i> indexes [<i>I</i> >= 2σ(<i>I</i>)]	<i>R</i> ₁ = 0.0435, <i>wR</i> ₂ = 0.0728	<i>R</i> ₁ = 0.0282, <i>wR</i> ₂ = 0.0689	<i>R</i> ₁ = 0.0317, <i>wR</i> ₂ = 0.0603	<i>R</i> ₁ = 0.0131, <i>wR</i> ₂ = 0.0364
Final <i>R</i> indexes [all data]	<i>R</i> ₁ = 0.0989, <i>wR</i> ₂ = 0.0861	<i>R</i> ₁ = 0.0373, <i>wR</i> ₂ = 0.0727	<i>R</i> ₁ = 0.0452, <i>wR</i> ₂ = 0.0641	<i>R</i> ₁ = 0.0142, <i>wR</i> ₂ = 0.0371
Largest diff. peak / hole / e Å ⁻³	1.32 / -0.94	2.31 / -0.97	1.25 / -0.81	0.70 / -0.83

Compound	9 (CCDC 1403015)	10 (CCDC 1403013)	11 (CCDC 1403017)	12 (CCDC 1403016)
Empirical formula	C ₅₅ H ₇₉ AgCl ₈ F ₃ N ₃ O ₃ P ₂ RuS	C ₆₁ H ₈₃ AgCl ₈ F ₃ N ₃ O ₃ P ₂ RuS	C ₃₇ H ₆₆ AuCl ₃ P ₂ Ru	C ₇₆ H ₁₃₄ AuBCl ₁₀ F ₄ P ₄ Ru ₂
Formula weight	1473.77	1549.93	977.28	2012.13
Temperature / K	122(2)	122(2)	122(2)	122(2)

Crystal system	triclinic	triclinic	monoclinic	monoclinic
Space group	<i>P</i> -1	<i>P</i> -1	<i>P</i> 2 ₁ / <i>c</i>	<i>P</i> 2/ <i>c</i>
<i>a</i> / Å	14.2480(9)	13.2970(6)	13.392(2)	19.988(4)
<i>B</i> / Å	15.8140(18)	14.5500(13)	17.6830(10)	16.619(4)
<i>c</i> / Å	16.6070(18)	18.9060(17)	20.172(2)	27.233(4)
α / °	70.503(9)	111.639(7)	90.000(9)	90.000
β / °	74.933(5)	93.007(5)	121.735(11)	100.779(15)
γ / °	68.534(9)	92.517(6)	90.000(7)	90.000
<i>V</i> / Å ³	3241.9(5)	3387.4(5)	4062.7(8)	8887(3)
<i>Z</i>	2	2	4	4
ρ_{calc} / g cm ⁻³	1.510	1.517	1.598	1.504
μ / mm ⁻¹	1.005	0.959	4.279	2.402
2 θ range for data collection / °	2.64 to 74.1	2.32 to 59.98	6.16 to 79.96	6.06 to 50.16
Reflections collected	152499	138841	198726	283877
Independent reflections	32982 [<i>R</i> _{int} = 0.0602]	19455 [<i>R</i> _{int} = 0.0480]	25013 [<i>R</i> _{int} = 0.1014]	15670 [<i>R</i> _{int} = 0.1295]
Restraints / parameters	0 / 694	0 / 748	0 / 397	0 / 884
Goodness-of-fit on <i>F</i> ²	1.065	1.092	1.241	1.224
Final <i>R</i> indexes [<i>I</i> >= 2 σ (<i>I</i>)]	<i>R</i> ₁ = 0.0605, <i>wR</i> ₂ = 0.1373	<i>R</i> ₁ = 0.0521, <i>wR</i> ₂ = 0.1405	<i>R</i> ₁ = 0.0521, <i>wR</i> ₂ = 0.1189	<i>R</i> ₁ = 0.0676, <i>wR</i> ₂ = 0.1546
Final <i>R</i> indexes [all data]	<i>R</i> ₁ = 0.0921, <i>wR</i> ₂ = 0.1571	<i>R</i> ₁ = 0.0670, <i>wR</i> ₂ = 0.1584	<i>R</i> ₁ = 0.0687, <i>wR</i> ₂ = 0.1298	<i>R</i> ₁ = 0.0831, <i>wR</i> ₂ = 0.1614
Largest diff. peak / hole / e Å ⁻³	2.58 / -2.63	2.54 / -2.04	4.01 / -3.35	2.45 / -1.38

Substitution kinetics in *cis*-PtCl₂(dms_o)₂. A solution of **RuC** (1.9 mg, 2.6 μ mol) in CD₂Cl₂ was added to a solution of *cis*-PtCl₂(dms_o)₂ (1.1 mg, 2.6 μ mol) in CD₂Cl₂, yielding a final volume of 0.9676 ml (1.314 g). The mixture was shaken immediately and mounted on a Bruker 500 MHz NMR machine. 180 s after mixing, 33 consecutive ¹H-NMR spectra were recorded. The integrals (s) from the dms_o ligands coordinated in *cis*-PtCl₂(dms_o)₂ were scaled to produce an intercept at *t* = 0 s corresponding to the initial concentration of *cis*-PtCl₂(dms_o)₂ (2.7 mM) in a plot of the inverse concentration versus time. The slope from the linear fit corresponds to the second-order rate constant, *k*₂ = 0.27(3) M⁻¹ s⁻¹. The data from the 1st and 23rd measurement (marked with gray, see Figure S 16) were excluded from the data treatment.

Supporting figures

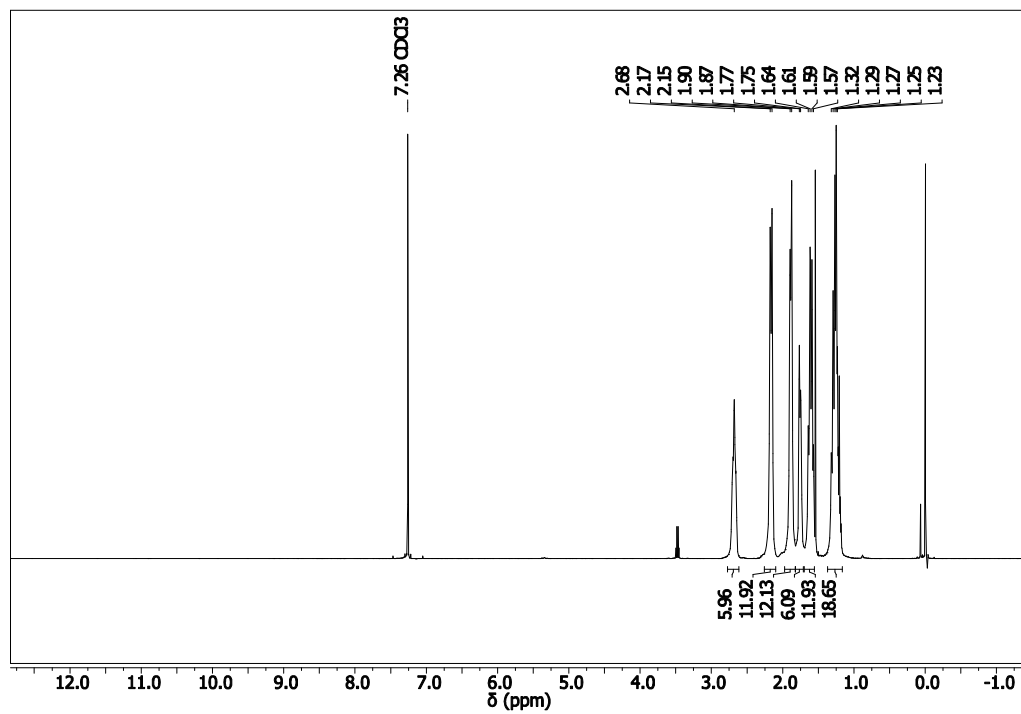


Figure S 1: ¹H-NMR of **11**. The quartet at 3.48 stems from a trace of diethyl ether.

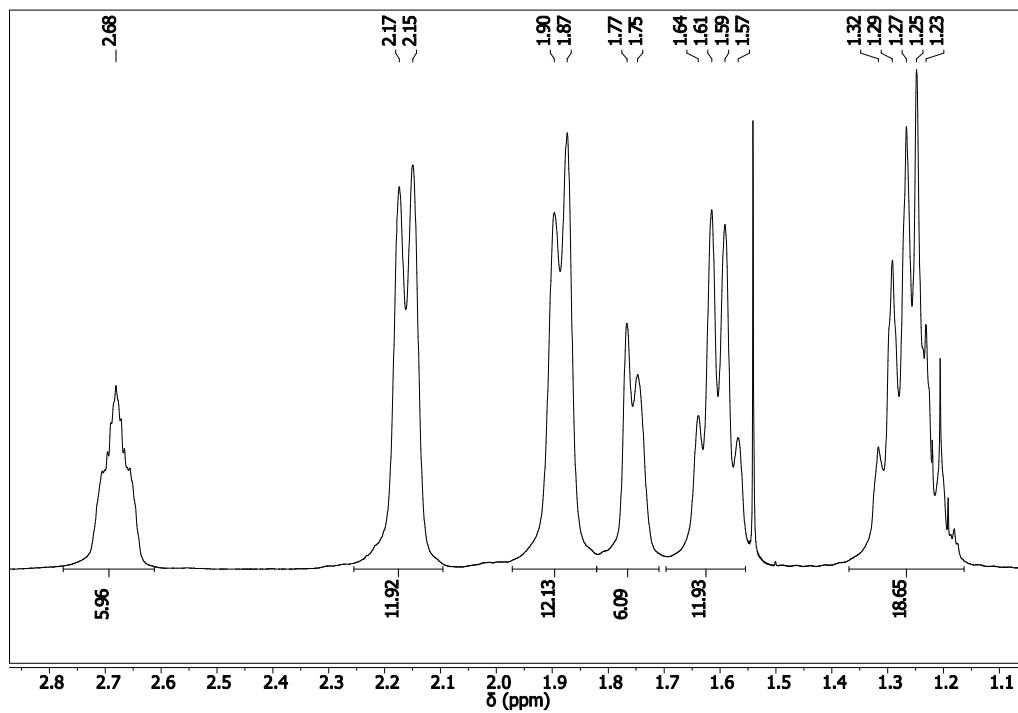


Figure S 2: ^1H -NMR of **11**, zoom. The singlet at 1.56 ppm stems from a trace of water in the solvent.

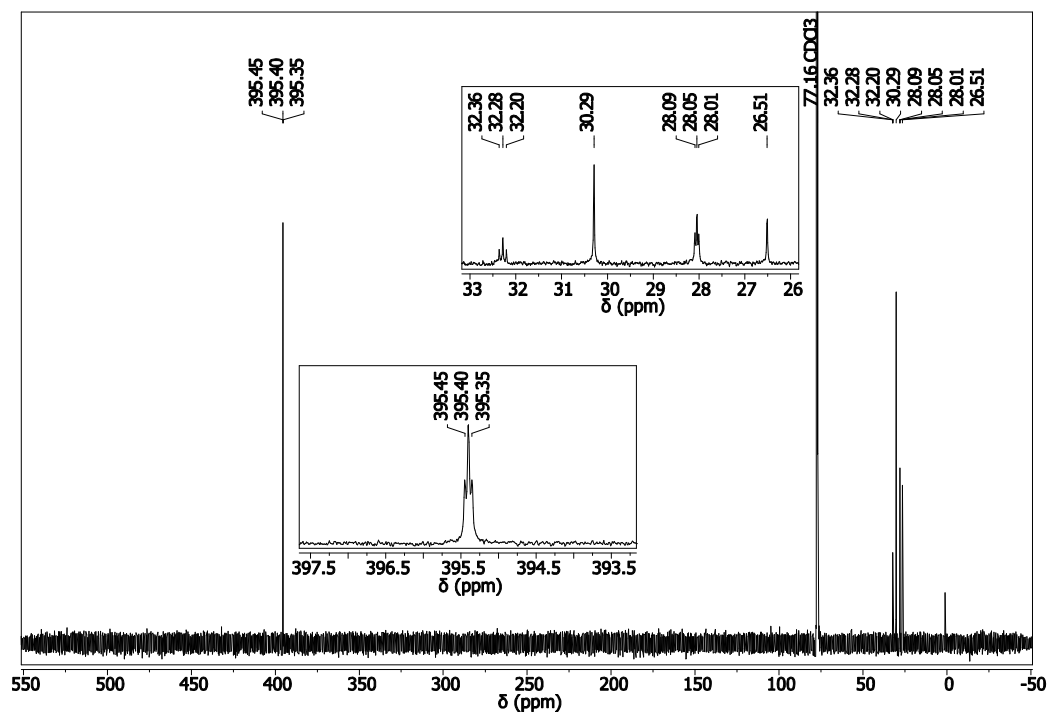


Figure S 3: $^{13}\text{C}\{^1\text{H}\}$ -NMR of **11**.

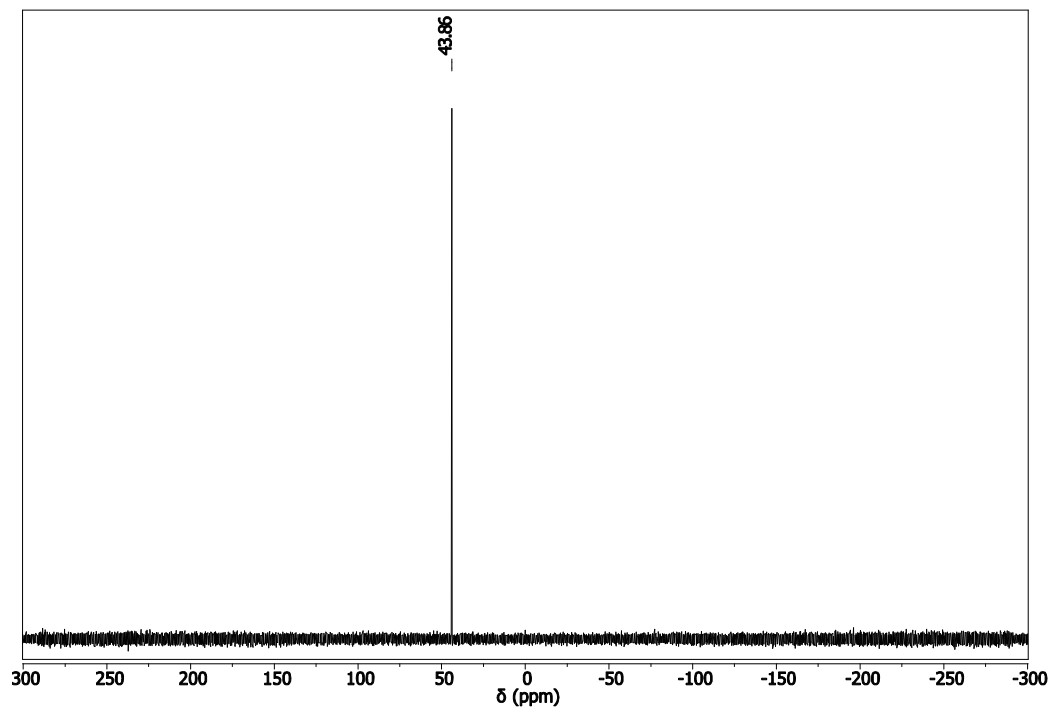


Figure S 4: $^{31}\text{P}\{^1\text{H}\}$ -NMR of 11.

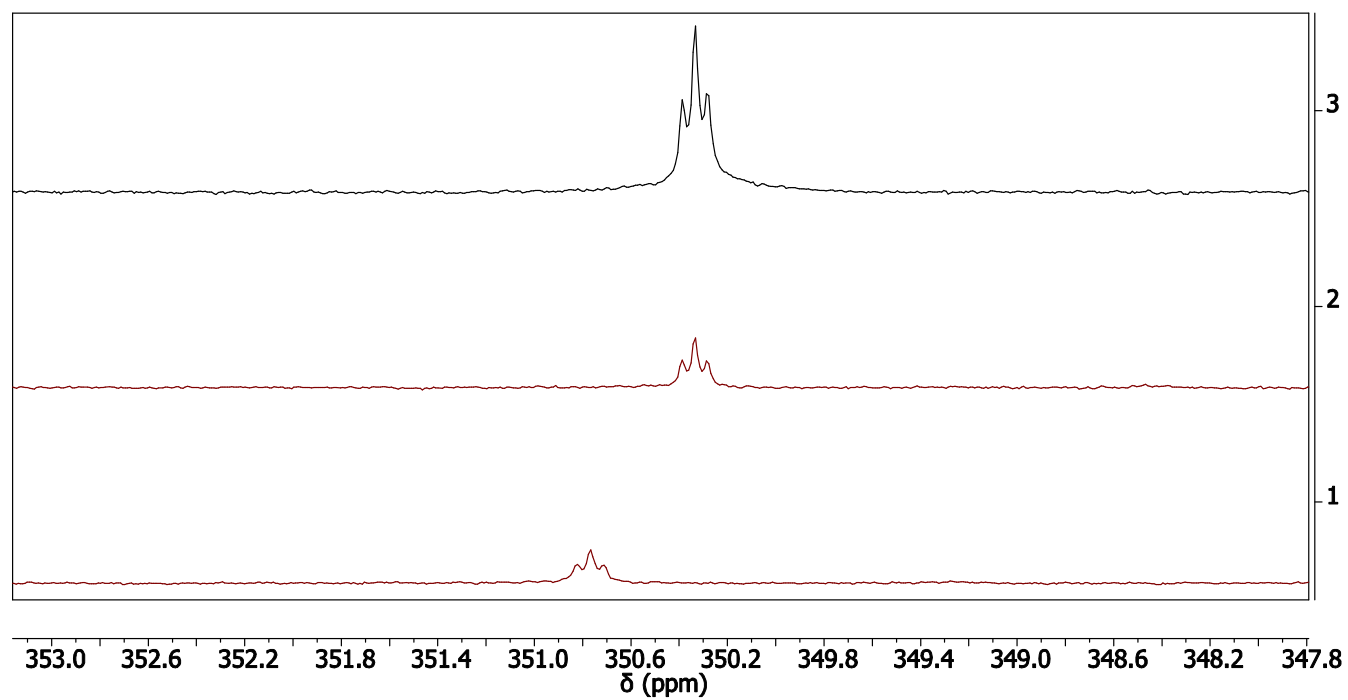


Figure S 5: $^{13}\text{C}\{^1\text{H}\}$ -NMR signals, carbide bridge region. 1) 6, 2) 6 and 2 eq. pyridine, 3) 7.

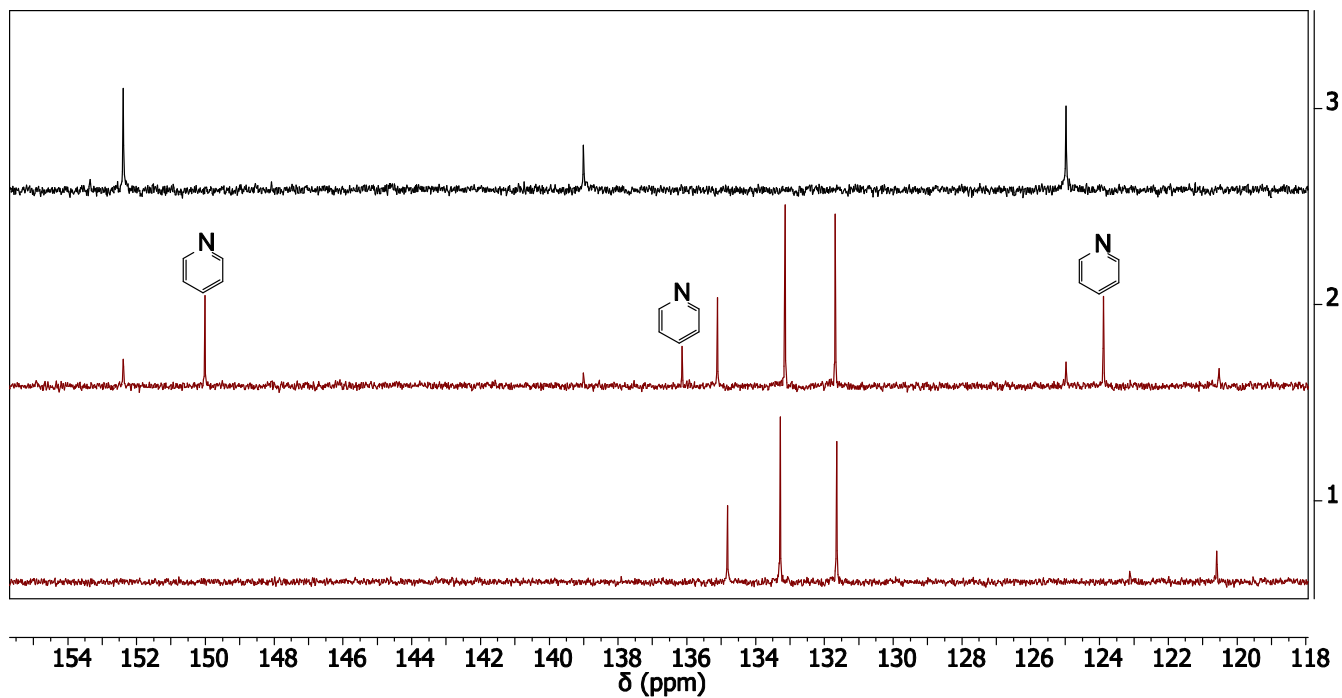


Figure S 6: $^{13}\text{C}\{^1\text{H}\}$ -NMR signals, aromatic region. 1) **6**, resonances arise from AsPh_4^+ . 2) **7** formed in the reaction between **6** and two equivalents of pyridine. The resonances arise from AsPh_4^+ (cf. spectrum 1), coordinated pyridine (cf. spectrum 3) and free pyridine (marked with skeletal formulae). 3) **7**, resonances arise from coordinated pyridine.

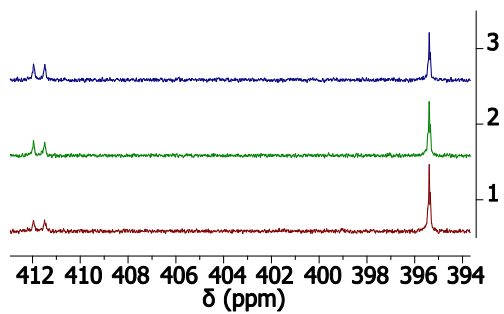


Figure S 7: reaction of **11** with $[\text{RhCl}(\text{cod})]_2$. Spectra 1, 2, and 3 are recorded after 1, 2, and 7 days.

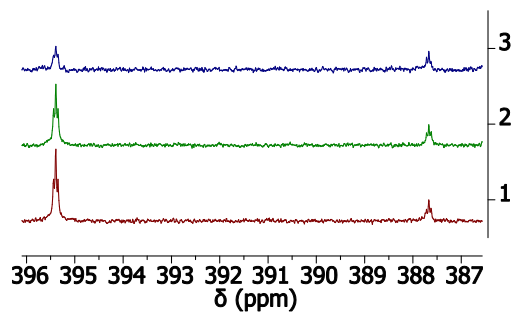


Figure S 8: reaction of **11** with $[\text{IrCl}(\text{cod})]_2$. Spectra 1, 2, and 3 are recorded after 1, 2, and 7 days.

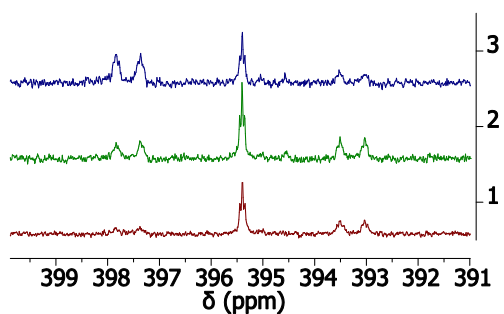


Figure S 9: reaction of **11** with $[\text{RhCl}(\text{CO})_2]_2$. Spectra 1, 2, and 3 are recorded after 1, 2, and 7 days.

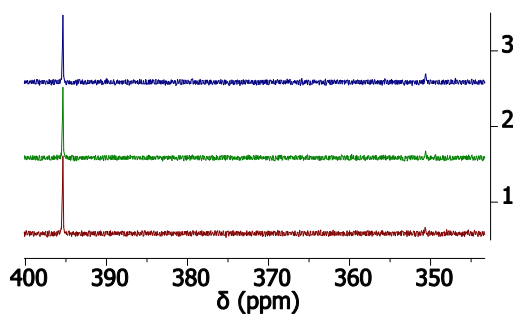


Figure S 10: reaction of **11** with $(\text{AsPh}_4)[\text{PtCl}_3(\text{C}_2\text{H}_4)]$. Spectra 1, 2, and 3 are recorded after 1, 2, and 7 days.

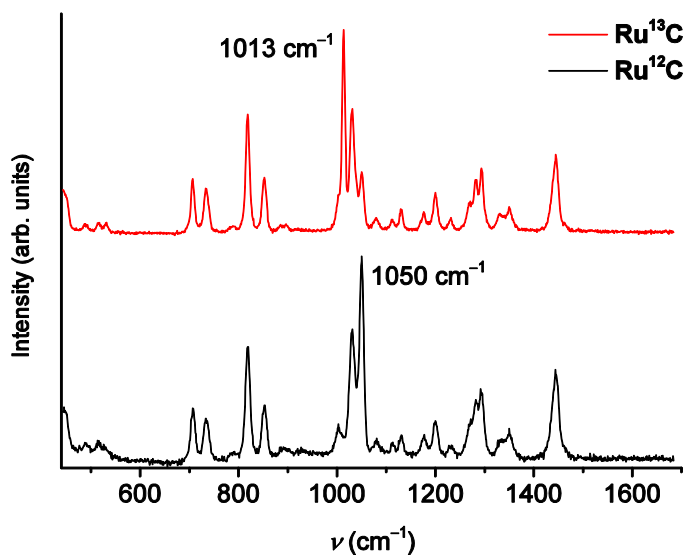


Figure S 11: Raman spectra of **RuC**.

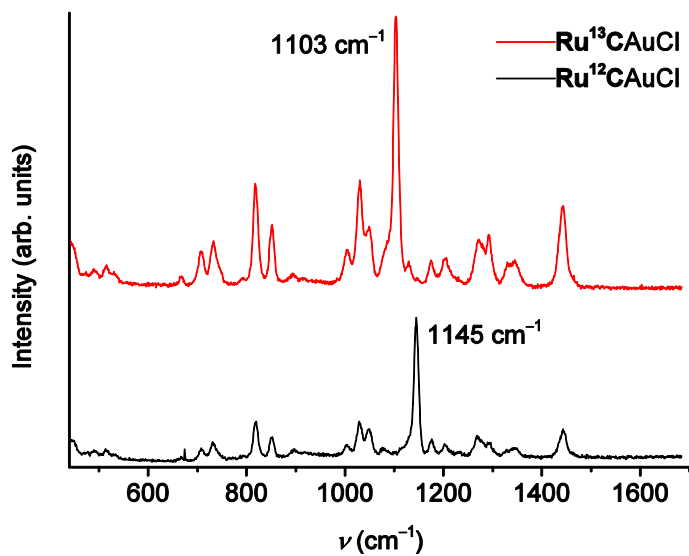


Figure S 12: Raman spectra of **11**.

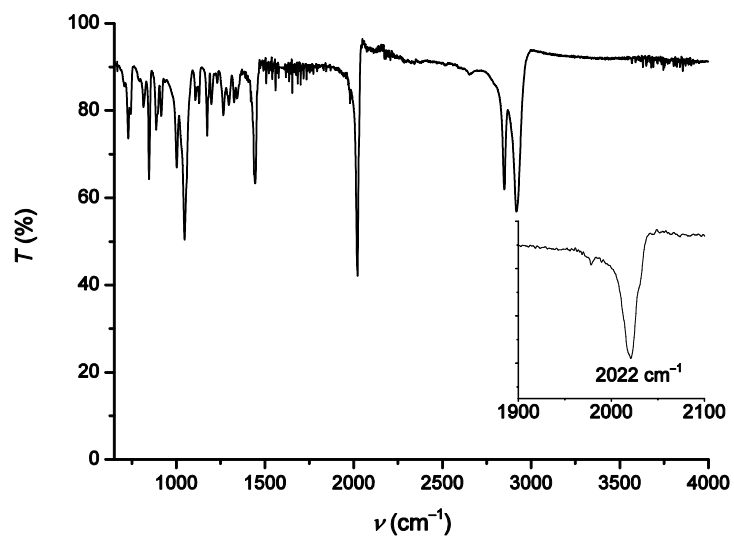


Figure S 13: IR spectrum of 3.

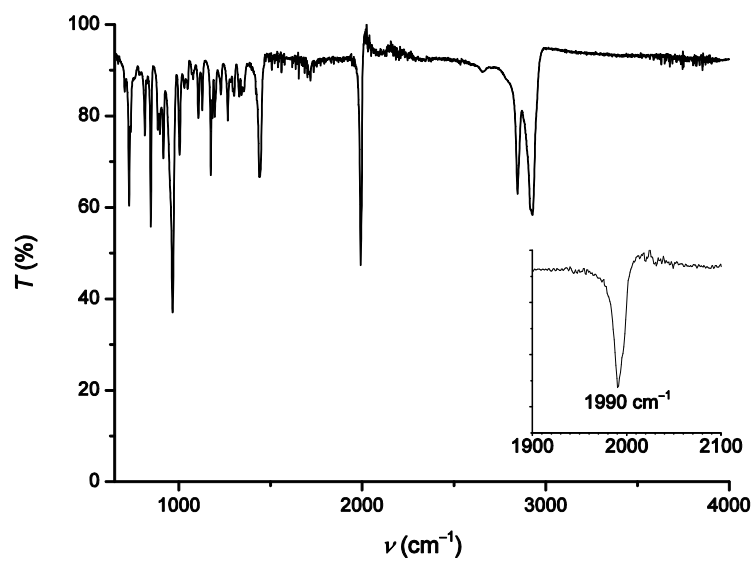


Figure S 14: IR spectrum of 4.

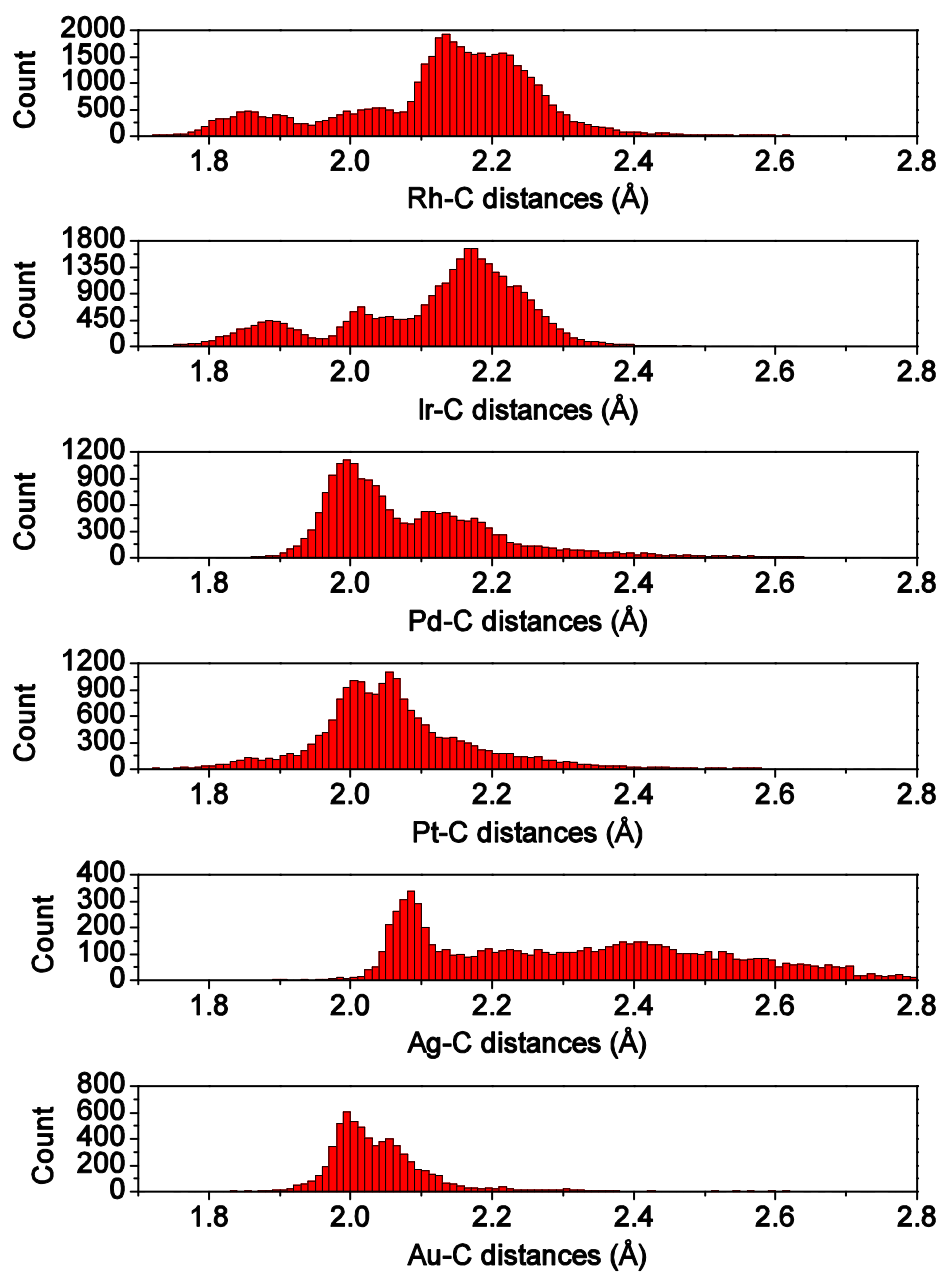


Figure S 15: histograms with M-C distances (M = Rh, Ir, Pd, Pt, Ag, Au) from the CSD v. 1.16.

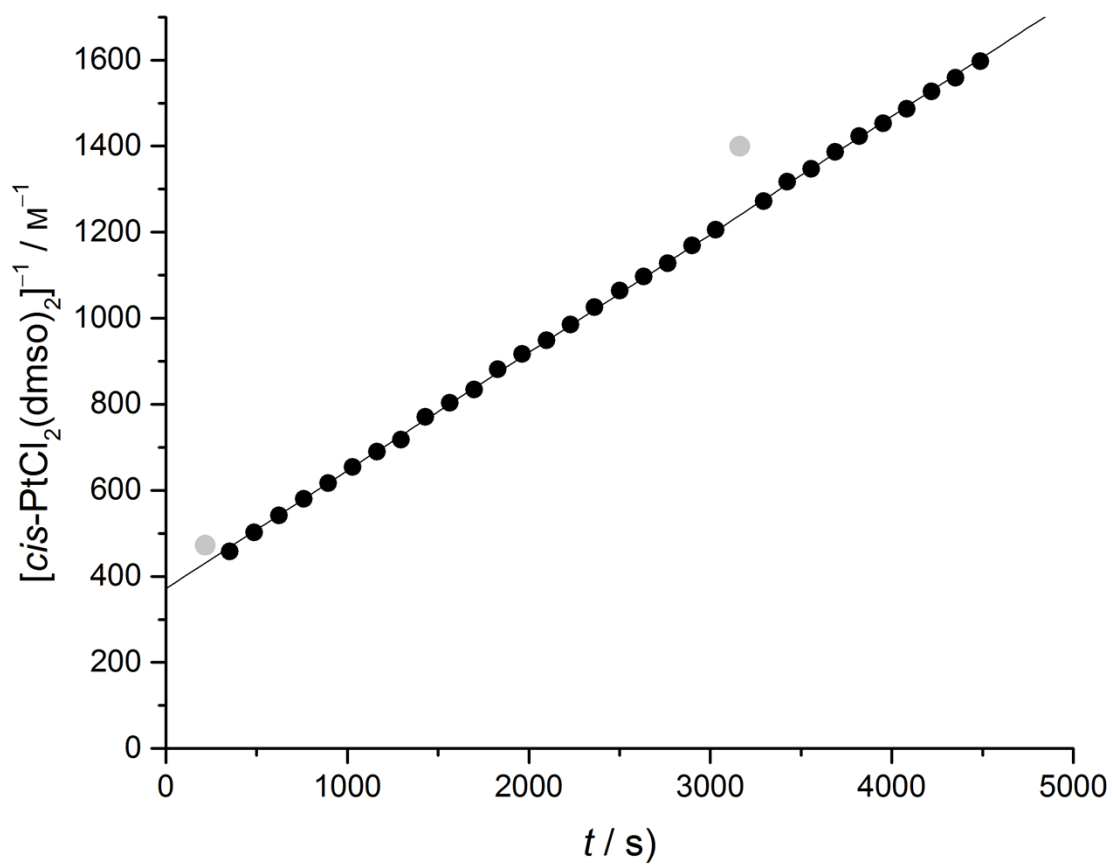


Figure S 16: Kinetics of dmsO substitution in *cis*-PtCl₂(dmsO)₂.

References

1. S. R. Caskey, M. H. Stewart, J. E. Kivela, J. R. Sootsman, M. J. A. Johnson and J. W. Kampf, *J. Am. Chem. Soc.*, 2005, **127**, 16750-16751.
2. G. Giordano, R. H. Crabtree, R. M. Heintz, D. Forster and D. E. Morris, in *Inorg. Synth.*, John Wiley & Sons, Inc., 1979, vol. 19, pp. 218-220.
3. J. L. Herde, J. C. Lambert, C. V. Senoff and M. A. Cushing, in *Inorg. Synth.*, John Wiley & Sons, Inc., 1974, vol. 15, pp. 18-20.
4. J. A. McCleverty, G. Wilkinson, L. G. Lipson, M. L. Maddox and H. D. Kaesz, in *Inorg. Synth.*, John Wiley & Sons, Inc., 1966, vol. 8, pp. 211-214.
5. H.-C. Böttcher and P. Mayer, *Z. Anorg. Allg. Chem.*, 2013, **639**, 234-236.
6. S. J. Lokken and D. S. Martin, *Inorg. Chem.*, 1963, **2**, 562-568.
7. P. J. Busse, B. Greene, M. Orchin, R. Zahray and J. Doyle, in *Inorg. Synth.*, John Wiley & Sons, Inc., 1980, vol. 20, pp. 181-185.
8. V. Y. Kukushkin, A. J. L. Pombeiro, C. M. P. Ferreira, L. I. Elding and R. J. Puddephatt, in *Inorg. Synth.*, 2002, vol. 33, pp. 189 – 196.
9. Z. Ma, Y. Xing, M. Yang, M. Hu, B. Liu, M. F. C. Guedes da Silva and A. J. L. Pombeiro, *Inorg. Chim. Acta*, 2009, **362**, 2921-2926.
10. R. Uson, A. Laguna, M. Laguna, D. A. Briggs, H. H. Murray and J. P. Fackler, in *Inorg. Synth.*, John Wiley & Sons, Inc., 1989, vol. 26, pp. 85-91.
11. M. I. Bruce, B. K. Nicholson, O. B. Shawkataly, J. R. Shapley and T. Henly, in *Inorg. Synth.*, John Wiley & Sons, Inc., 1989, vol. 26, pp. 324-328.
12. J. H. MacNeil, P. K. Gantzel and W. C. Trogler, *Inorg. Chim. Acta*, 1995, **240**, 299-304.
13. R. Uson, J. Fornies, M. Tomas, I. Ara, J. M. Casas and A. Martin, *J. Chem. Soc., Dalton Trans.*, 1991, DOI: 10.1039/DT9910002253, 2253-2264.
14. *COLLECT, Nonius BV: Delft, The Netherlands, 1999.*
15. A. J. M. Duisenberg, L. M. J. Kroon-Batenburg and A. M. M. Schreurs, *J. Appl. Crystallogr.*, 2003, **36**, 220-229.
16. G. Sheldrick, *Acta Crystallographica Section A*, 1990, **46**, 467-473.
17. G. Sheldrick, *Acta Crystallographica Section A*, 2008, **64**, 112-122.
18. *Bruker; Bruker AXS, Inc. SAINT, Version 7.68A; Bruker AXS: Madison, WI, 2009.*
19. G. Sheldrick, *SADABS, Version 2008/2; University of Göttingen: Germany, 2003.*
20. O. V. Dolomanov, L. J. Bourhis, R. J. Gildea, J. A. K. Howard and H. Puschmann, *J. Appl. Crystallogr.*, 2009, **42**, 339-341.
21. L. J. Bourhis, O. V. Dolomanov, R. J. Gildea, J. A. K. Howard and H. Puschmann, *Acta Crystallographica Section A*, 2015, **71**, 59-75.